

# Ammonia Emissions from Swiss Agriculture and their Effects on Atmospheric Chemistry and Ecosystems

Christof Ammann<sup>a\*</sup> and Alex Valach<sup>b</sup>

**Abstract:** Ammonia (NH<sub>3</sub>) is an important atmospheric pollutant due to its contribution to secondary inorganic aerosol formation and its deposition and impacts on (semi-)natural ecosystems. Therefore various efforts have been made to limit emissions to the atmosphere. The predominant emission source in Switzerland is livestock agriculture, wherein NH<sub>3</sub> is volatilised from ammonium contained in animal manure. While modelled NH<sub>3</sub> emissions based on agricultural activity data indicate a minor decrease since 2000, concentration measurements do not reflect this trend. This can at least partly be attributed to a decline in the transformation of NH<sub>3</sub> to particulate ammonium due to significantly decreased emission of oxidised nitrogen and sulfur compounds in the past decade. The partitioning between the gaseous and the particulate phase also determines the deposition pathway (dry or wet deposition) and thus the average lifetime and transport distance in the atmosphere. Gaseous NH<sub>3</sub> is subject to fast dry deposition and is deposited preferentially to ecosystems close to the source. Once deposited into an ecosystem, NH<sub>3</sub> leads to eutrophication and acidification of water and soils, which change the plant community composition and microbial functioning, especially in N-sensitive ecosystems. Although NH<sub>3</sub> can also cause direct toxicity to plants, assessments of ecosystem impacts are generally collated using the critical load approach, which includes the input of all N compounds. These reveal that in 2020, 87% of forests, 94% of raised bogs, 74% of fens, and 42% of dry mountain grasslands likely experienced adverse impacts from N exceedances in Switzerland. To improve this situation, considerable NH<sub>3</sub> emission abatement efforts are needed in the future.

**Keywords:** Ammonia · Critical loads · Dry and wet deposition · Emission · Secondary inorganic aerosols



**Christof Ammann** is a senior scientist at the Swiss Federal Research Institute Agroscope and leads the research team on agricultural greenhouse gas emissions. His interdisciplinary research focuses on field measurements of the exchange of reactive and non-reactive trace gases between the biosphere and the atmosphere using various measurement techniques. From 2012 to

2023, he was a member of the Swiss Federal Commission on Air Hygiene—the clean air advisory board of the Swiss Government.



**Alex Valach** combined his studies in Ecology with a PhD in Atmospheric Chemistry from Lancaster University to investigate ecosystem-atmosphere interactions of reactive and non-reactive trace gas fluxes. Postdoctoral projects at the University of California, Berkeley and at Agroscope Zürich aimed at understanding ecosystem functioning driving fluxes to develop land management practices for climate change

mitigation. Having recently joined the *Gaseous Emissions from Agriculture* group at the Bern University of Applied Sciences his work now focusses on livestock emissions and their impacts with the aim to improve emission abatement methods.

## 1. Introduction

Ammonia (NH<sub>3</sub>) is the most abundant alkaline component in the atmosphere and constitutes one of the most reactive nitrogen (N) species. It is considered an atmospheric pollutant due to its adverse effects on N-sensitive ecosystems and contribution to the formation of fine particulate matter<sup>[1]</sup> associated with adverse human health outcomes.<sup>[2,3]</sup> Agriculture produces 86% of NH<sub>3</sub> emissions to the atmosphere globally,<sup>[4]</sup> while its contribution regionally can reach even higher values as is the case in Switzerland.<sup>[5,6]</sup> A large part of the NH<sub>3</sub> emitted to the atmosphere is ultimately deposited in gaseous form or *via* precipitation to (semi-)natural ecosystems. This implies a considerable nutrient loss from agricultural production, but more importantly an inadvertent excess N input to sensitive and partly protected ecosystems including forests, wetlands, and lakes. There, it may lead to eutrophication and soil acidification resulting in biodiversity loss.<sup>[7,8]</sup> Through its impact on N and carbon cycling, the exchange of greenhouse gases can also be affected.<sup>[9,10]</sup> Following the UNECE Gothenburg Protocol,<sup>[11]</sup> considerable efforts have been initiated since the 1990's to decrease anthropogenic emissions of nitrogenous compounds in Europe. However, while the emission of oxidised N compounds (mainly NO<sub>x</sub> from combustion processes) and the corresponding atmospheric concentrations have decreased in Switzerland by half over the last 20 years, the reduction of NH<sub>3</sub> emissions has been only moderate and has not been fully reflected in observed concentrations.<sup>[6,14]</sup>

This review mainly focusses on the specific situation and research activities in Switzerland concerning processes governing the emission of NH<sub>3</sub> from agriculture, its subsequent transport and transformations in the atmosphere, and resulting impacts in N-sensitive ecosystems.

\*Correspondence: Dr. C. Ammann, E-mail: christof.ammann@agroscope.admin.ch  
<sup>a</sup>Agroscope; <sup>b</sup>Bern University of Applied Sciences

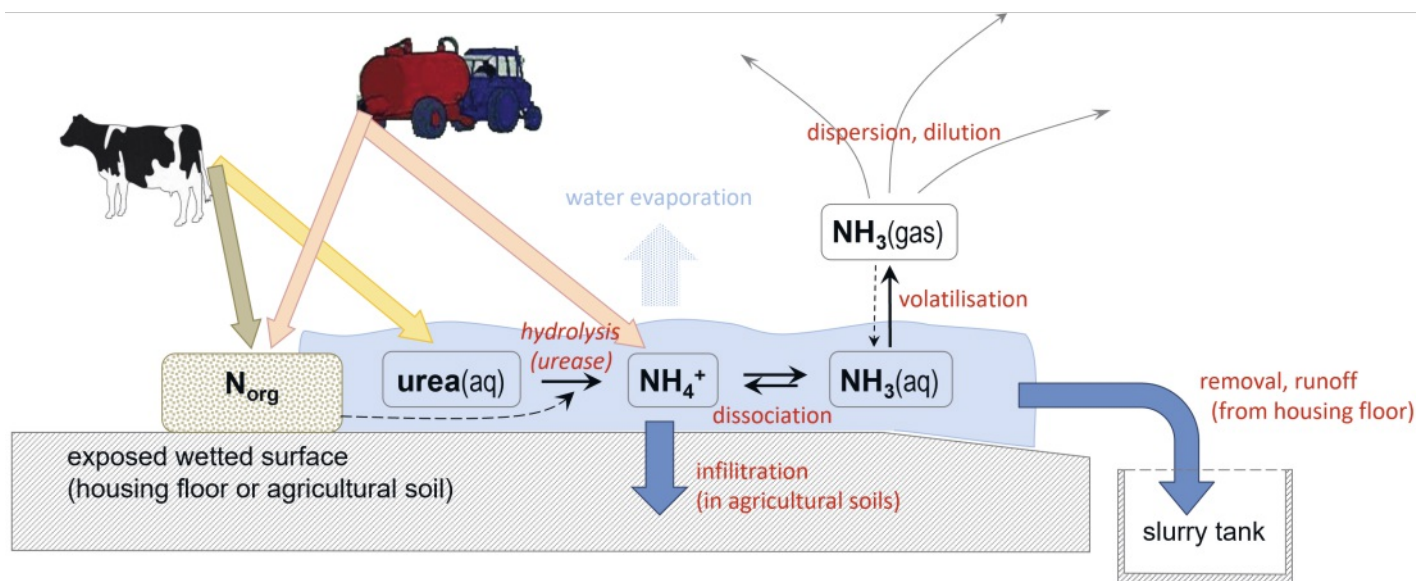


Fig. 1. Schematic illustration of processes controlling the emission of  $\text{NH}_3$  from its primary source, livestock agriculture.

## 2. Ammonia Emissions from Agriculture

### 2.1 Emission Sources

In 2022, agriculture produced 94% of  $\text{NH}_3$  emissions in Switzerland,<sup>[6]</sup> of which 93% resulted from livestock farming. Animals (cattle, pigs, poultry, etc.) excrete N in urine (ca. 50–70%, mainly in the molecular form of urea) and dung (ca. 30–50%, mainly in solid organic forms). Once deposited on animal housing floors or pasture surfaces and catalysed by the urease enzyme in the dung or soil, urea is rapidly hydrolysed and equilibrates with aqueous  $\text{NH}_3$  depending on pH and temperature (Fig. 1). The  $\text{NH}_3(\text{aq})$  is in equilibrium with the gas phase according to Henry's law. Since the volatilised  $\text{NH}_3$  is usually dispersed and rapidly diluted in the air, the volatilisation can persist until the pH in the aqueous phase is reduced which favours  $\text{NH}_4^+$ . This  $\text{NH}_3$  volatilisation process occurs similarly from soiled surfaces in livestock housings as well as from manure surfaces during storage and after field application. Due to the fast transformation in the aqueous phase, the water-soluble N compounds urea,  $\text{NH}_4^+$ , and  $\text{NH}_3(\text{aq})$  are often quantified together as total ammoniacal N (TAN). The particulate organic N of the excreted dung and constituent of slurry shows a low chemical reactivity and little exchange with the TAN fraction.

### 2.2 Concentration and Flux Measurements

In order to investigate and quantify the exchange of  $\text{NH}_3$  between sources (and sinks, see Sect. 4) at the surface and the atmosphere, accurate concentration and flux measurements are necessary. A traditional and relatively simple approach uses the reactivity and water solubility of  $\text{NH}_3$  by trapping/scrubbing it from the air into an acidified liquid solution or surface coating either by an active sample air flow (e.g. impinger<sup>[12]</sup> or denuder<sup>[13]</sup>) or by passive gas diffusion (passive samplers<sup>[14]</sup>) over time periods of hours to weeks. The trapping solution or coating is then brought to the lab for chemical or photometric analysis. However, this approach is labour intensive and unsuitable for continuous measurements with high time resolutions. Continuously operating online gas analysers are usually closed-path spectroscopic instruments using inlet tubing and particle filters to protect the measurement cell. However, due to its water-soluble characteristics,  $\text{NH}_3$  adsorbs readily to most surfaces including the inner walls and filters of inlet systems and analysers. While this is less problematic for

instance with high concentrations close to strong sources (e.g. within animal housings<sup>[15]</sup>), it is more problematic for medium to low ambient concentrations.

One solution to this problem is the use of open-path *in situ* spectroscopic instruments measuring the optical absorption of infrared or UV-light sources (such as lasers or lamps) over absorption path lengths of tens to a few hundred meters.<sup>[16]</sup>

For  $\text{NH}_3$  emissions from agricultural fields after manure application or during grazing, various flux measurement techniques are available<sup>[17]</sup> and have been applied in Switzerland in the past decades, including wind tunnels,<sup>[18]</sup> integrated horizontal flux approaches,<sup>[18]</sup> inversed dispersion methods,<sup>[12,16,19,20]</sup> aerodynamic gradient method,<sup>[21]</sup> and eddy covariance.<sup>[22]</sup> Except for the wind tunnels, the listed approaches are based on micrometeorological principles and make use of natural atmospheric turbulent transport near the surface, without altering the ambient environmental conditions.

Although representing the largest local  $\text{NH}_3$  sources, emissions from animal housings are complex to quantify, as they encompass multiple heterogeneous sources, depositing surfaces, variable gas exchange rates depending on the ventilation method, and structures that affect atmospheric turbulence. Closed structures with controlled ventilation are suited to indirect gas balancing methods, whereby the emissions are calculated from indoor and outdoor concentration differences and precise air exchange rates. This is less feasible for open structures with natural ventilation,<sup>[23]</sup> which are prevalent in Switzerland. Another approach is the tracer ratio method, *i.e.* the controlled release of an inert tracer gas inside the structure with concentration measurements inside or outside the building to determine the ratio between the released gas and  $\text{NH}_3$ , which is assumed to also represent the ratio of emission rates.<sup>[23]</sup>

A method that operates at high time resolutions for longer periods without the need for in-house installations is the inverse dispersion method.<sup>[24]</sup> It is based on concentration measurements up- and downwind of the structure combined with a backward dispersion model to simulate the diffusion between the emission source and measurement location.<sup>[25]</sup>

### 2.3 Emission Modelling and National Inventory

From the available experimental studies in Switzerland and internationally, mean emission factors (*i.e.*  $\text{NH}_3$  emitted as a fraction of TAN) for the different stages of the manure cascade

(Fig. 2) are derived, depending on animal category, farm system, production method, *etc.* These are used together with agricultural activity data in the Agrammon emission model<sup>[26,27]</sup> to derive annual  $\text{NH}_3$  emissions from agriculture for the Swiss national inventory. The main emission sources in livestock production are animal housings and exercise yards (36%), slurry and solid manure storage (11% and 6%, respectively), their application to fields (34% and 10%, respectively), and grazing (3%).<sup>[5]</sup>

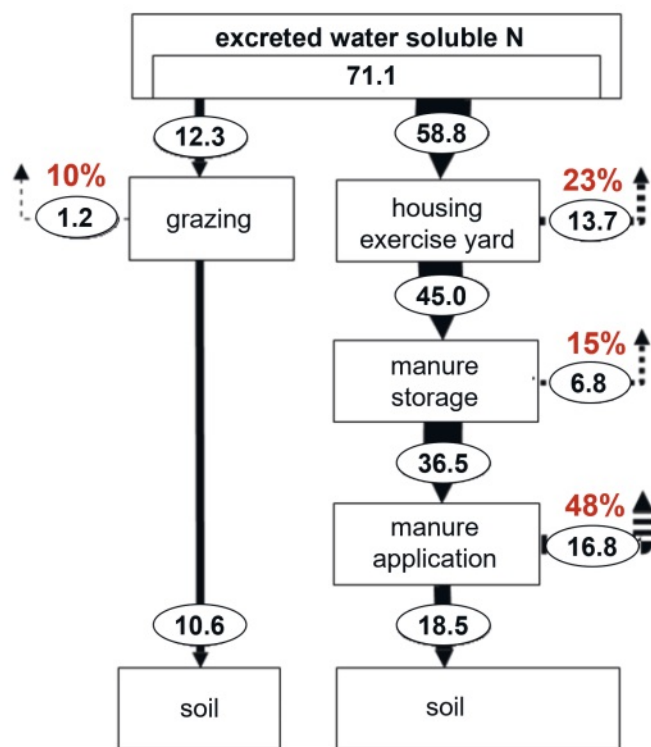


Fig. 2. Fate of N in Swiss livestock production after excretion in animal housings or during grazing. Black values represent flows of water-soluble TAN (urea /  $\text{NH}_4^+$  /  $\text{NH}_3(\text{aq})$ ; see Fig. 1) in  $\text{kt N yr}^{-1}$  through the manure management cascade. The dotted arrows indicate losses of  $\text{NH}_3$  to the atmosphere, with the red numbers (in percent) indicating the corresponding emission factors (*i.e.* the relative loss) in the respective cascade step. Numbers are for the year 2020, from ref. [5].

The emission factors and resulting emissions are subject to considerable uncertainties, because they are based on a limited number of international experimental studies and do not yet include all recent findings (*e.g.* experimental studies found significantly lower  $\text{NH}_3$  emission factors for slurry spreading under Swiss conditions than presently used<sup>[5,12]</sup>). In addition to the total livestock-related  $\text{NH}_3$  emissions of  $38.5 \text{ kt N yr}^{-1}$  (the sum of all emission pathways in Fig. 2), there are also synthetic fertiliser-related emissions from plant production ( $2.8 \text{ kt N yr}^{-1}$ ) and non-agricultural emissions ( $2.4 \text{ kt N yr}^{-1}$ ) that represent minor contributions to the total emissions of  $43.7 \text{ kt N yr}^{-1}$ . As part of the inventory, annual emissions are also quantified in a spatially-resolved emission map with a  $100 \text{ m} \times 100 \text{ m}$  grid resolution.<sup>[28,29]</sup>

## 2.4 Emission Mitigation Measures and Temporal Trends

Measures to mitigate agricultural  $\text{NH}_3$  emissions to the atmosphere try to reduce or inhibit the reaction and equilibration chain in Fig. 1 that leads to  $\text{NH}_3$  volatilisation. Since the emission occurs at the surface of the liquid phase, an effective measure is to reduce the surface area of the TAN-containing liquid exposed to the atmosphere. For the field application of slurry, this is achieved by using band spreading techniques (trailing hose, trailing shoe)

that reduce the exposed surface by 75-80%, which consequently lowers  $\text{NH}_3$  emissions by 30-50% compared to simple broadcast spreading.<sup>[12]</sup> Another measure is the dilution of slurry by adding water before spreading. This leads to reduced TAN concentrations in the higher application volume and thus enhances the fraction of slurry that rapidly infiltrates into the soil. As indicated by Fig. 2, grazing generally produces lower  $\text{NH}_3$  emissions than keeping the animals in housings, which could be observed in field experiments.<sup>[20]</sup> This is because urine, containing most of the excreted TAN, is deposited in small, confined patches on the pasture leading to fast infiltration into the soil. Within animal housings,  $\text{NH}_3$  emissions can be reduced by facilitating a fast runoff of urine into a (closed) storage tank and by regular removal of the solid manure such as with a frequently operated automatic scraper. The emission from slurry tanks is effectively diminished by a cover that reduces the air exchange and dispersion into the atmosphere.

Another emission mitigation option is the acidification of slurry by adding acids (mainly  $\text{H}_2\text{SO}_4$ ) to lower the pH and inhibit the dissociation of  $\text{NH}_4^+$  to  $\text{NH}_3$  (Fig. 1). Naturally ventilated housings can reduce volatilisation from lower temperatures during the cold season, but conversely lead to higher emissions due to the more efficient air exchange that reduces the headspace concentration and facilitates volatilisation. This also causes higher emissions in the warm season compared to closed housings with limited mechanical ventilation. An effective mitigation method is a reduction of protein, the main N source in animal feed, as this leads to significantly lower excretion of soluble N and thus to less  $\text{NH}_3$  emissions along the entire manure management cascade.<sup>[20,30]</sup> A detailed survey of best available techniques for preventing and reducing ammonia emissions from agricultural sources has been published by the UNECE executive body for the Convention on Long-range Transboundary Air Pollution.<sup>[31]</sup>

Between 1990 and 2000,  $\text{NH}_3$  emissions decreased by about 1% per year. This can mainly be attributed to a reduction in animal numbers and a substantial increase in grazing activity (with reduced emissions<sup>[20,31]</sup>) during that period. Afterwards, between 2000 and 2020, the reduction was smaller at only 0.6% per year despite increased propagation and incentives for the implementation of abatement measures. The emission reductions were partly offset by the increase in animal-friendly housing systems, which provide a larger surface area per animal, but also produce a trade-off of higher  $\text{NH}_3$  emissions.<sup>[27]</sup> Band spreading (or incorporation) and slurry tank covers, have recently become mandatory for most farmers in Switzerland, and new technical measures are being developed but need to be tested in scientific projects. Historical time series of  $\text{NH}_3$  emissions since 1750 have been reconstructed for various regions and countries worldwide including Switzerland.<sup>[32]</sup> They show that the  $\text{NH}_3$  emissions in Switzerland one hundred years ago were about 30% lower than today and reached a maximum around 1980 when animal numbers peaked.

Table 1: Annual surface-atmospheric  $\text{NH}_x$  exchange budgets for Switzerland including total anthropogenic  $\text{NH}_3$  emissions<sup>[5,6]</sup> and the different deposition pathways of  $\text{NH}_3$  and  $\text{NH}_4^+$ <sup>[29]</sup> in units of  $\text{kt N yr}^{-1}$

	1990	2000	2010	2020
Emissions $\text{NH}_3$	56.3 (100%)	50.1 (100%)	47.5 (100%)	43.7 (100%)
Dry deposition $\text{NH}_3$	21.6 (38%)	19.3 (39%)	19.0 (40%)	23.9 (55%)
Dry deposition $\text{NH}_4^+$	2.2 (4%)	2.2 (4%)	1.8 (4%)	1.2 (3%)
Wet deposition $\text{NH}_4^+$	24.2 (43%)	21.3 (43%)	17.3 (36%)	16.4 (38%)
Deposition $\text{NH}_x$ total	47.9 (85%)	42.8 (85%)	38.1 (80%)	41.5 (95%)

### 3. Atmospheric Transport and Transformation

#### 3.1 Processes and Lifetimes

Agricultural  $\text{NH}_3$  emissions enter the atmospheric boundary layer that comprises the lowest 100–1000 m of the atmosphere. The boundary layer is vertically well mixed and thus closely coupled to the terrestrial surface, while the exchange with the overlying free troposphere is relatively slow. Therefore,  $\text{NH}_3$  can easily re-deposit onto the surface by dry deposition (Fig. 3), which leads to a short atmospheric lifetime of emitted  $\text{NH}_3$  of only a few hours.<sup>[33,34]</sup> An alternative and potentially faster process is the conversion to  $\text{NH}_4^+$  in particulate matter (aerosols) through reactions with atmospheric acids, mainly nitric and sulfuric acid. This results in secondary inorganic aerosols (SIA) that have a longer lifetime in the atmosphere of a few days on average. This is because their deposition to the surface is much slower than for the gaseous  $\text{NH}_3$  molecules. Consequently, SIA containing  $\text{NH}_4^+$  can reach the free troposphere, where they are transported with the mean wind over longer distances. The main removal process for particulate  $\text{NH}_4^+$  is wet deposition by rain and snowfall.<sup>[1]</sup> Compared to these deposition processes, the oxidation of  $\text{NH}_3$  to  $\text{NO}$  and  $\text{N}_2\text{O}$  by reaction with  $\text{OH}$  is very slow (chemical lifetime of several weeks<sup>[35]</sup>) and thus can be neglected for the atmospheric  $\text{NH}_3$  budget.

The effectiveness of the removal of  $\text{NH}_3$  and aerosols from the atmosphere by surface dry deposition can be described by the deposition velocity  $V_{d,s}$  that is defined as the factor between the (negative) deposition flux  $F_s$  and the near surface concentration  $C_s$  of species  $s$ :

$$F_s = -V_{d,s} \times C_s \quad (1)$$

For gaseous  $\text{NH}_3$ , average deposition velocities range between 10 and 30  $\text{mm s}^{-1}$  over vegetated surfaces and are thus one order of magnitude higher than the corresponding values for SIA of 1 to 2.5  $\text{mm s}^{-1}$ .<sup>[28]</sup> Due to the slow deposition velocity and hence longer atmospheric lifetime,  $\text{NH}_4^+$  can be transported over long distances.

The effectiveness of wet deposition of particulate  $\text{NH}_4^+$  depends on the occurrence and type of clouds and precipitation events.

The equilibrium of the reversible transformation of  $\text{NH}_3$  to particulate  $\text{NH}_4^+$  depends on the ratio between  $\text{NH}_x$  (the sum of  $\text{NH}_3$  and  $\text{NH}_4^+$ ) and the acidic reaction partners ( $\text{HNO}_3$  and  $\text{H}_2\text{SO}_4$  or their ions  $\text{NO}_3^-$  and  $\text{SO}_4^{2-}$ ) as well as on the concentration of other metal ions, the liquid water content and temperature.<sup>[36,37]</sup> It can be calculated for a specified air volume by a thermodynamic equilibrium model like ISORROPIA.<sup>[38]</sup> Using this model, a study from 2006 with data from Payerne showed that the atmospheric boundary layer on the Swiss Plateau was over-saturated with  $\text{NH}_3$  and therefore the particle concentration was only weakly dependent on changes in  $\text{NH}_3$  concentrations.<sup>[39]</sup> While a lowering of  $\text{NH}_3$  emissions by 25% only led to a decrease of SIA by 1–5%, an  $\text{NH}_3$  reduction of more than 50% was needed to decrease SIA production by >10%.

For a more comprehensive investigation of the interaction and partitioning between the different transport, transformation, and removal processes in the atmosphere and their effects on the spatial distribution of  $\text{NH}_3$  and  $\text{NH}_4^+$  over Switzerland and Europe, three-dimensional dynamic atmospheric chemistry and transport models (CTM) are employed.<sup>[40–42]</sup> These exhibited that the aerosol formation in Switzerland was only weakly sensitive to  $\text{NH}_3$  during summer and only slightly more so in winter, while  $\text{NO}_x$  emissions (leading to the formation of  $\text{HNO}_3/\text{NO}_3^-$ ) from traffic, industry, and domestic heating were more generally a leading cause. Since Swiss  $\text{NO}_x$  emissions have decreased considerably in the past decades<sup>[6,29]</sup> but  $\text{NH}_3$  emissions declined only slightly, this sensitivity of aerosol formation to  $\text{NO}_x$  (representing the limiting factor) even increased in the past decades and probably will continue to in the future.<sup>[42]</sup>

#### 3.2 Concentrations Monitoring

To monitor near-surface concentrations of  $\text{NH}_3$  in Switzerland, a network of passive sampler stations has been installed over the past 20 years by national and cantonal authorities.<sup>[14]</sup> It grew from 13 permanent sites (presently still in operation) to over 100 sites in recent years. The samplers yield average concentrations over two

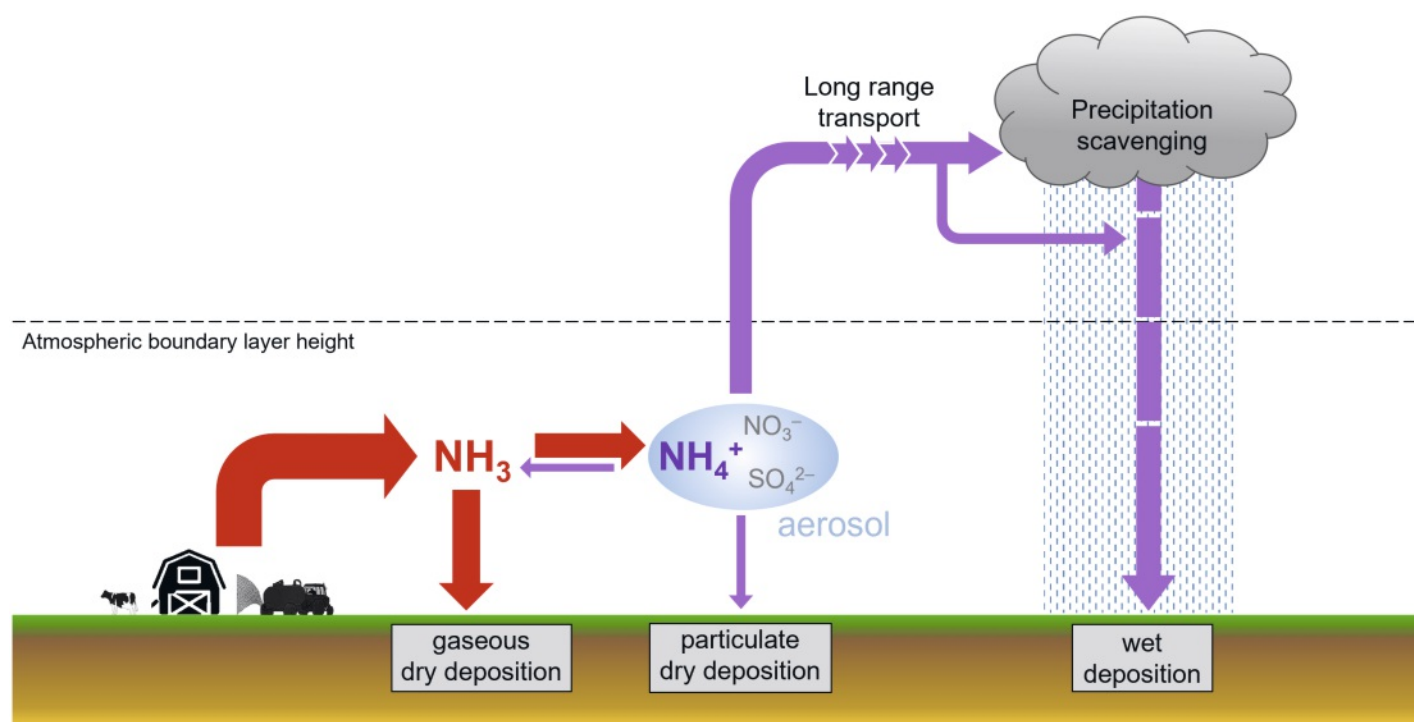


Fig. 3. Schematic illustration of the fate of emitted  $\text{NH}_3$  in the atmosphere. The width of the arrows gives a rough indication of the quantitative importance of the processes in Switzerland.

or four weeks. They exhibit a high spatial variability with annual mean concentrations between 0.5 and 12  $\mu\text{g m}^{-3}$ , that mainly reflect the proximity of the monitoring site to intensive agriculture. A seasonal pattern can be observed from monthly measurements and especially in regions with a high livestock density, the concentrations follow agricultural activities with lowest values in winter and highest in spring and late autumn, when slurry application is widespread. The passive sampler networks were supposed to monitor the effect of  $\text{NH}_3$  emission reduction measures. However, while the national emission inventory indicates a 13% reduction of emissions between the years 2000 and 2020, most of the passive sampler monitoring sites showed no significant change or even an increase in average  $\text{NH}_3$  concentrations.<sup>[43]</sup> This discrepancy could be explained by the reduction of the acidic compounds (mostly in the form of nitric and sulfuric acids) during the same time and thus a decreasing transformation to particulate  $\text{NH}_4^+$ . A part of the effect may also be attributed to the temperature increase due to climate warming and its positive impact on  $\text{NH}_3$  volatilisation<sup>[44]</sup>, which has not been considered hitherto in the emission inventory (Sect. 2.3).

An additional recently developed option for monitoring the larger scale spatial distribution and temporal trends of atmospheric  $\text{NH}_3$  levels are total column observations by satellites,<sup>[4,34]</sup> assumed to mainly represent  $\text{NH}_3$  concentrations in the lower boundary layer.<sup>[33]</sup>

## 4. Surface Deposition

### 4.1 Deposition Measurements

The quantification of N deposition from the atmosphere to terrestrial surfaces is generally separated into two contrasting process pathways according to dry and wet deposition (see Fig. 3 and Sect. 3.1). This applies to modelling (Sect. 4.2) as well as to measurements, on which model parameters are based. The dominant species for dry deposition is  $\text{NH}_3$ , but the following methods similarly apply to particulate  $\text{NH}_4^+$ , as well as to oxidised N compounds. The simplest experimental approach to quantify dry deposition is the inferential method (Eqn. 1) that requires local concentration measurements and a more or less sophisticated and site-specific estimation of the deposition velocity.<sup>[13,45]</sup> This approach heavily relies on assumptions in the determination of the deposition velocity and, therefore, can be considered as an estimate derived from a combination of measurement and modelling. More direct measurements of  $\text{NH}_3$  deposition have been performed using micrometeorological approaches (see also Sect. 2.2) such as the aerodynamic gradient method<sup>[46-49]</sup> and, more recently, the eddy covariance method.<sup>[50,51]</sup> With a time resolution of typically one hour, these methods allow an investigation of seasonal and diurnal variations and dependencies on surface vegetation and weather conditions. Yet, such measurements usually require greater infrastructure (mains power, measurement towers) and sophisticated instrumentation, which limits the application to few selected sites.

Wet deposition can be measured by analysing the concentration of the compounds of interest in accumulated precipitation samples. While wet-only samplers are closed by a moving lid between precipitation events, the simpler bulk deposition samplers are permanently open and thus include partial contributions of dry deposition as well.<sup>[52]</sup> A sampler positioned below a forest canopy measures the so-called throughfall deposition. This process also samples the substances deposited during dry periods on the foliage and washed off during subsequent precipitation, hence it may be considered to represent the sum of wet and dry deposition. However, it has been found that throughfall N deposition is systematically lower than total N deposition (determined from wet deposition samplers and dry deposition by the inferential method),<sup>[53,54]</sup> which can be explained e.g. with stomatal and cuticular uptake of  $\text{NH}_3$  and  $\text{NH}_4^+$  by tree leaves<sup>[55]</sup>

and possibly by microbial N processing on plant surfaces. The average relationship between total deposition and throughfall could be described by an empirical power function, yet with considerable scatter,<sup>[52]</sup> and is likely to be highly site and species dependent.

### 4.2 Modelling of Spatially Distributed Deposition

To quantify the spatial distribution of N deposition to (semi-) natural ecosystems and to assess the exceedance of critical N loads (see Sect. 5.2) within Switzerland, a semi-empirical diagnostic model approach was developed.<sup>[28,29]</sup> We refer to it here as the ‘SND model’ (abbreviated for: Swiss Nitrogen Deposition model) and briefly describe it. Deposition maps with a resolution of 500 m x 500 m were produced for 1990 and since 2000 generated every five years and include the following compounds: wet and dry deposition of ammonium ( $\text{NH}_4^+$ ) and nitrate ( $\text{NO}_3^-$ ) as well as gaseous deposition of ammonia ( $\text{NH}_3$ ), nitrogen dioxide ( $\text{NO}_2$ ) and nitric acid ( $\text{HNO}_3$ ).

For dry deposition of  $\text{NH}_3$ , the spatial distribution of near surface concentrations was determined in a first step. For this purpose, the SND model combines a spatially resolved  $\text{NH}_3$  emission inventory with a statistical dispersion model (source-receptor relationship) as a function of distance up to 50 km from the source taking prevailing wind directions into account. The raw model concentrations are compared to measured concentrations from passive sampler networks (representing 80 sites across Switzerland in 2020)<sup>[14]</sup> and an empirical topography-dependent correction factor is applied. This correction showed a considerable trend from 2010<sup>[28]</sup> to 2015<sup>[56]</sup> and further to 2020,<sup>[29]</sup> wherein the measured  $\text{NH}_3$  concentrations increased relative to the emission-related raw model values. This trend is in line with the finding of the decreased transformation of  $\text{NH}_3$  to  $\text{NH}_4^+$ .<sup>[43]</sup> Concentrations of particulate  $\text{NH}_4^+$  and  $\text{NO}_3^-$  in the SND model are derived from mapped secondary particulate matter multiplied by the average observed relative contents of 15% and 22%, respectively. In the second step, the annual average concentrations maps for  $\text{NH}_3$  and  $\text{NH}_4^+$  are multiplied with the deposition velocities for different land cover classes<sup>[28]</sup> to obtain annual dry deposition fluxes (see Sect. 3.1) for each grid cell.

For wet deposition, the available monitoring data from the National Air Pollution Monitoring Network<sup>[57]</sup> and the long-term forest ecosystem monitoring network<sup>[53,58]</sup> in Switzerland for  $\text{NH}_4^+$  and  $\text{NO}_3^-$  concentrations in precipitation are used to derive altitude dependent relationships that are combined with gridded annual precipitation maps. Finally, the total N deposition map (Fig. 4) is produced from the sum of the different deposition pathways. The resulting N deposition pattern is relatively similar to the  $\text{NH}_3$  emission map with generally high values in the area of the Central Swiss Plateau and northern Pre-Alps, especially in the central and north-eastern regions with intensive livestock agriculture, and lowest values in the Alps. The spatial patterns were comparable to the results of a CTM model for 2006,<sup>[41,59]</sup> although the latter had a lower resolution (ca. 5 km x 5 km). The high total N deposition south of the Alps can be attributed to higher (advected) concentrations of oxidised species from the Po valley.

The spatially integrated annual deposition values of the SND model for the different pathways are listed in Table 1 with their temporal development. The total  $\text{NH}_x$  deposition is 5% to 20% smaller than the  $\text{NH}_3$  emission, which represents a good agreement considering the uncertainties of both modelled values due to assumptions and simplifications. In addition, a somewhat lower deposition amount could be explained by a net export of particulate  $\text{NH}_4^+$  to neighbouring countries.<sup>[60]</sup> Concerning the different deposition pathways,  $\text{NH}_3$  dry deposition has superseded wet deposition as the most important contributor between 2000 and 2010. This trend is consistent with the findings of the reduced transformation to particulate  $\text{NH}_4^+$  discussed in Sect. 3. However,

the CTM model results<sup>[59]</sup> for 2006 indicated a two times higher dry deposition than wet deposition. This might have partly been due to its different, more complex dynamic modelling of the dry deposition. The co-operative programme for monitoring and evaluation of the long-range transmission of air pollutants in Europe (EMEP) uses a CTM model to routinely calculate the transport and deposition of  $\text{NH}_x$  and other pollutants over all of Europe. It is based on the same emission data but indicates a considerably lower total  $\text{NH}_x$  deposition for Switzerland of only 34 kt  $\text{N yr}^{-1}$  for 2020 compared to the SND (Table 1), implying a larger net  $\text{NH}_x$  export to neighbouring countries.<sup>[61]</sup>

#### 4.3 Uncertainties and Improvements in Dry Deposition Modelling

The uncertainty of model results is generally difficult to quantify. Modelled near-surface concentrations of  $\text{NH}_3$  and other compounds can be validated with measured passive sampler concentrations from monitoring networks. In the CTM model study by Aksyoglu and Prévôt,<sup>[59]</sup> no overall systematic deviation but relatively large differences for individual sites were observed. Such an independent validation was not possible for the SND model, because the same data were already used for its calibration (Sect. 4.2). Accordingly, the model showed no systematic deviation but still a considerably high relative root mean squared error of 43% for individual sites.<sup>[28]</sup> For both models, these uncertainties may be explained by their limited spatial resolution in comparison to point measurements and the high short-range variability of  $\text{NH}_3$  due to its short lifetime.

Another limitation of the SND model is the use of annual mean  $V_d$  values for the main land-cover classes. Since very few multi-annual measurements of  $\text{NH}_3$  dry deposition fluxes are available, the derivation of representative annual values is difficult, and they may not account for (anti-)correlations between  $\text{NH}_3$  concentrations and deposition velocity at the diurnal and seasonal scales. Therefore, process-based deposition modelling can be a suitable alternative because the deposition is disaggregated into subprocesses driven by environmental parameters. Multiple resistance models of dry deposition<sup>[62]</sup> also used in CTMs<sup>[59]</sup> include dependencies on wind speed and surface roughness as well as resistance parameters for separate stomatal, cuticular and soil deposition under wet and dry conditions. These process-specific parameters can be calibrated with limited direct flux measurement data.

An additional complex factor that has been known for a long time but not frequently implemented in deposition models for  $\text{NH}_3$  is the ‘compensation point’.<sup>[63,64]</sup> It represents the surface emission potential and, in relation to the atmospheric concentration, determines the direction of the  $\text{NH}_3$  flux (*i.e.* deposition or emission).

Emission potentials depend on leaf and soil N or  $\text{NH}_4^+$  contents making parameterisations highly ecosystem-specific. Due to a lack of data for parameterisations, models often do not include the compensation point, but this may lead to an overestimation of the mean deposition when atmospheric concentrations are low.<sup>[65]</sup>

## 5. Impacts on Ecosystems

### 5.1 Investigation of Impacts

About 50% of the atmospheric  $\text{NH}_x$ , mostly resulting from agricultural  $\text{NH}_3$  emissions, is deposited to natural or semi-natural ecosystems in Switzerland including forests, (semi-)natural dry grasslands, wetlands, and lakes.<sup>[10,29]</sup> Among these, forests cover by far the largest area (75%) and are distributed over all parts of Switzerland. However, the research and reporting on the effects of enhanced N inputs to ecosystems generally considers the total reactive N load and not specific N forms or deposition pathways. This is partly because specific experiments with controlled dry deposition (*i.e.* gaseous fumigation) of  $\text{NH}_3$ <sup>[66,67]</sup> are difficult to perform and thus uncommon. Instead, N is typically added in liquid solution – resembling wet deposition – in most experiments although this may be less detrimental to ecosystems than dry  $\text{NH}_3$  deposition<sup>[66]</sup> and hence does not properly represent impacts experienced by ecosystems. In Switzerland, the  $\text{NH}_x$  compounds (as listed in Table 1) contribute on average about 70% to the total N deposition while the other 30% are oxidized N compounds ( $\text{NO}_2$ ,  $\text{HNO}_3$ ,  $\text{NO}_3^-$ ).<sup>[29,59]</sup>

The impact of N deposition to (semi-)natural ecosystems depends on the input rate and on the N-sensitivity of the ecosystem. Increased N input can act as fertilizer and enhance plant growth, but in excess leads to eutrophication. This alters the competitive relationship between species, which can cause a loss of biodiversity especially in ecosystems adapted to nutrient-poor conditions.<sup>[68,69]</sup> Deposited N contributes to soil acidification due to nitrification of  $\text{NH}_4^+$  and nitrate leaching with percolation water. This also accelerates the leaching of cations ( $\text{Ca}^{2+}$ ,  $\text{K}^+$ ,  $\text{Mg}^{2+}$ ) from the system leading to nutrient deficiencies.<sup>[70]</sup> In forests, these effects can cause unbalanced nutrition,<sup>[71,72]</sup> increased vulnerability to storms,<sup>[73]</sup> changes in the composition of beneficial mycorrhiza,<sup>[74-76]</sup> increase and decrease of growth<sup>[77,78]</sup> and impact on tree crown condition.<sup>[79]</sup> The processing of the additional N in the soil produces increased emissions of the potent greenhouse gas  $\text{N}_2\text{O}$ . In the national greenhouse gas inventory, these additional emissions are attributed to the original N source, *i.e.* the agricultural sector, and are therefore denoted as indirect  $\text{N}_2\text{O}$  emissions. They account for 20% of the total  $\text{N}_2\text{O}$  emissions in Switzerland.<sup>[10]</sup>

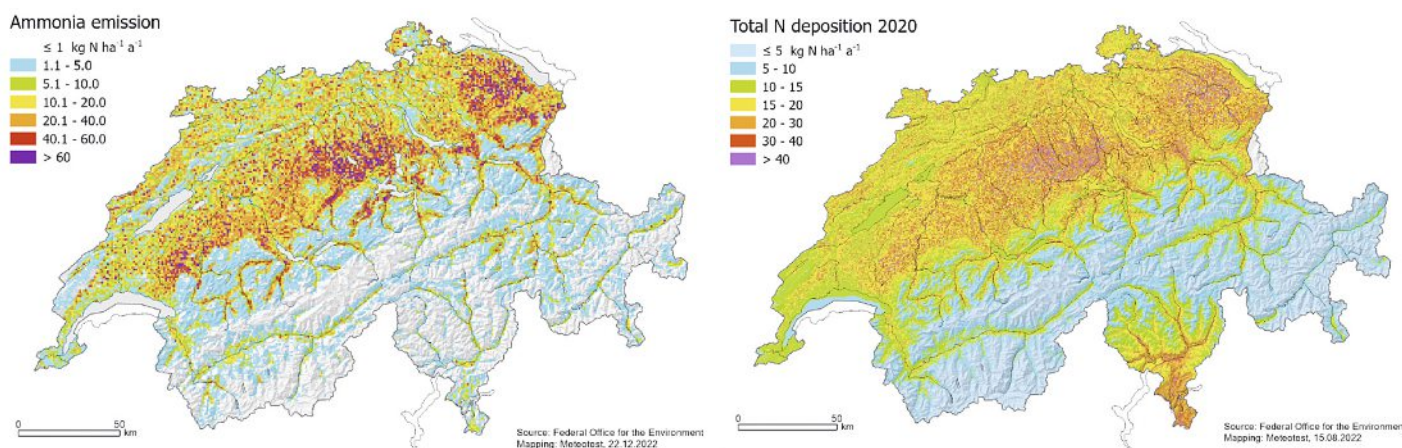


Fig. 4. Maps of annual  $\text{NH}_3$  emission and total N deposition, both in  $\text{kg N ha}^{-1} \text{yr}^{-1}$ , for 2020 in Switzerland (Source: Federal Office for the Environment, ref. [29]).

## 5.2 Critical Loads and Critical Levels

To characterize the sensitivity of (semi-)natural ecosystems to inputs of N and other pollutants, thresholds using a critical loads (CL) approach were developed within the UNECE Convention on Long-Range Transboundary Air Pollution and are regularly updated according to current scientific knowledge.<sup>[80]</sup> These values are defined as annual inputs of a pollutant, below which no significant harmful effects occur. They were determined based on results from scientific field studies with N addition experiments, from field observation studies along N deposition gradients, mesocosm studies, simple mass balance approaches, but also incorporating expert judgement.<sup>[81–83]</sup> For total N, the CL values range between 4 and 20 kg N ha<sup>-1</sup> yr<sup>-1</sup> for Swiss ecosystems.<sup>[29]</sup> By combining the CL values with vegetation and soil information as well as the modelled annual N deposition map (see Sect. 4.2), a CL exceedance map for Switzerland is periodically produced.<sup>[28,29]</sup> The map for 2020 showed that at 87% of forest sites the CL for total N was exceeded, and similarly large shares of the protected areas of raised bogs (94%) and fens (74%) showed exceedances. For species-rich dry grassland the value was lower (42%), because they are mainly situated in the Alps and thus more distant from intensive agriculture. A recent review of observations at monitoring stations in Switzerland supported these modelled results.<sup>[84]</sup>

An alternative ‘critical level’ concept also exists for NH<sub>3</sub> that indicates the (annual average) ambient concentration, above which sensitive plant species can be damaged by the direct toxicity from exposure to a gaseous pollutant in the air. The critical level for NH<sub>3</sub> is set at 3 µg m<sup>-3</sup> (with an uncertainty range of 2–4 µg m<sup>-3</sup>) for higher plants, including forest trees and grassland species and only 1 µg m<sup>-3</sup> for lichens and bryophytes.<sup>[80,85]</sup> As with the CL approach for total N input, the critical levels for exposure to NH<sub>3</sub> alone are also exceeded at a majority of monitoring sites at or near sensitive ecosystems in Switzerland, except for montane dry grasslands.<sup>[14]</sup> In contrast to other air pollutants like ozone, NO<sub>2</sub>, or particulate matter, the critical level for NH<sub>3</sub> has less legal/political impact. Because of the less substantial empirical evidence for critical levels of NH<sub>3</sub> as well as the overlap with the CL approach for total N deposition, the Swiss Federal Commission for Air Hygiene has recommended to give a general priority to the CL approach.<sup>[86]</sup>

## 6. Conclusions and Outlook

The processes governing the cycling of NH<sub>3</sub> in Switzerland from the agricultural emissions through atmospheric transport and transformation to dry and wet deposition back to the surface are relatively well known, although considerable quantitative uncertainties remain. Multi-year temporal trends in deposition pathways (dry vs. wet deposition) can be attributed to changes in emissions of oxidised N compounds and the resulting alterations in the partitioning between the gaseous and the particulate phase. However, because of interactions between the different NH<sub>3</sub> cycling processes, observed mean NH<sub>3</sub> concentrations seem to be barely capable of detecting interannual variations or moderate long-term trends in emissions. Yet, they represent the (mean) spatial distribution of NH<sub>3</sub> emissions fairly well, considering the short atmospheric lifetime and associated transport distances. Monitoring efforts with higher temporal resolutions in the order of one hour would allow a more detailed consideration of diurnal meteorological effects (such as calm conditions and shallow stable boundary layers during the night) on the average NH<sub>3</sub> concentrations.

The dry deposition process of NH<sub>3</sub> is highly variable in space and time not only due to the short lifetime of NH<sub>3</sub> but also due to the dependence of the deposition velocity on various meteorological and vegetation parameters. It is therefore still subject to high uncertainties, especially within short distances from the source, where the majority of NH<sub>3</sub> deposition takes place. In Switzerland, this issue is of special importance since most

N-sensitive ecosystems are close to agricultural emission sources due to the predominantly small-scaled agriculture with high livestock densities.

For a comprehensive investigation of the entire NH<sub>3</sub> cycle and its sensitivity to present and future climate change, a dynamic CTM type model with high spatial resolution coupled with high-resolution information about emission processes and vegetation conditions would be desirable. More detailed and accurate modelling also requires corresponding accurate and direct emission and deposition flux data for calibration of parameters and validation of outputs. This implies a need for more detailed flux measurements with high temporal resolutions. New commercially available instruments like the recently developed open-path laser-based instrument<sup>[87]</sup> may facilitate continuous direct flux measurements<sup>[88]</sup> with the eddy covariance method to observe emissions as well as dry deposition.

Currently, two Swiss research projects are in progress that link aspects of NH<sub>3</sub> emission, atmospheric processing, deposition, and impacts. The ETH domain joint initiative ReCLEAN (Reactive nitrogen at the CLimate, Energy, Agriculture, water, and health Nexus)<sup>[89]</sup> aims to “holistically understand and quantify nitrogen fluxes across and within compartments to predict the effects of energy transition and environmental changes from other drivers (climate change)”. It includes various research groups from across the ETH domain and encompasses the study of N cycling processes in the atmosphere, in natural and in agricultural soils and ecosystems, as well as in water bodies. The second, a SNF-funded Sinergia project, Follow’N’Flow (Following the Nitrogen Fluxes from agricultural Losses via deposition into Wetland ecosystems causing climate impacts),<sup>[90]</sup> will investigate localised small-scale processes that lead to excess N inputs from agricultural losses into N-sensitive ecosystems, as well as impacts on ecosystem functioning and subsequently on net ecosystem greenhouse gas balances. This includes the emission, short-range transport, and dry deposition processes of NH<sub>3</sub> using new technologies with the aim to inform and improve emission abatement and ecosystem protection measures.

## Acknowledgements

We thank Peter Waldner and Thomas Kupper for their valuable inputs during writing and editing of the manuscript.

Received: May 1, 2024

- [1] D. Fowler, K. Pilegaard, M. A. Sutton, P. Ambus, M. Ravionen, J. Duyzer, D. Simpson, H. Fagerli, S. Fuzzi, J.K. Schjoerring, C. Granier, A. Neftel, I.S.A. Isaksen, P. Laj, M. Maione, P.S. Monks, J. Burkhardt, U. Daemmgen, J. Neiryneck, E. PersonneR.J. Wichink Kruit, K. Butterbach-Bahl, C. Flechard, J.P. Tuovinen, M. Coyle, G. Gerosa, B. Loubet, N. Altimir, L. Gruenhage, C. Ammann, S. Cieslik, E. Paoletti, T.N. Mikkelsen, H. Ro-Poulsen, P. Cellier, J.N. Cape, L. Horvath, F. Loreto, U. Niinemets, P.I. Palmer, J. Rinne, P. Misztal, E. Nemitz, D. Nilsson, S. Pryor, M.W. Gallagher, T. Vesala, U. Skiba, N. Brüeggemann, S. Zechmeister-Boltenstern, J. Williams, C. O’Dowd, M.C. Facchini, G. de Leeuw, A. Flossman, N. Chaumerliac, J.W. Erisman, *Atmos. Environ.* **2009**, *43*, 5193, <https://doi.org/10.1016/j.atmosenv.2009.07.068>.
- [2] C. A. Pope, M. Ezzati, D. W. Dockery, *N. Engl. J. Med.* **2009**, *360*, 376, <https://doi.org/10.1056/NEJMsa0805646>.
- [3] J. Lelieveld, J. S. Evans, M. Fnais, D. Giannadaki, A. Pozzer, *Nature*, **2015**, *525*, 367, <https://doi.org/10.1038/nature15371>.
- [4] M. van Damme, L. Clarisse, B. Franco, M. A. Sutton, J. W. Erisman, R. W. Kruit, M. Van Zante, S. Whitburn, J. Hadji-Lazarou, D. Hurtmans, C. Clerbaux, P.-F. Coheur, *Environ. Res. Lett.* **2021**, *16*, 55017, <https://doi.org/10.1088/1748-9326/abd5e0>.
- [5] T. Kupper, C. Häni, D. Bretscher, F. Zaucker, ‘Ammoniakemissionen der schweizerischen Landwirtschaft 1990 bis 2020’, **2022**, [https://agrammon.ch/assets/Documents/Bericht\\_Agrammon\\_1990-2020\\_-20220331.pdf](https://agrammon.ch/assets/Documents/Bericht_Agrammon_1990-2020_-20220331.pdf).
- [6] Federal Office for the Environment FOEN, ‘Switzerland’s Informative Inventory Report 2024 (IIR)’, Submission under the UNECE Convention on Long-Range Transboundary Air Pollution. Submission

- of March 2024 to the United Nations ECE Secretariat, **2024**, <https://www.ceip.at/status-of-reporting-and-review-results/2024-submission>.
- [7] J. Aber, W. McDowell, K. Nadelhoffer, A. Magill, G. Berntson, M. Kamakea, S. McNulty, W. Currie, L. Rustad, I. Fernandez, *BioScience* **1998**, *48*, 921, <https://doi.org/10.2307/1313296>.
- [8] R. Bobbink, K. Hicks, J. Galloway, T. Spranger, R. Alkemade, M. Ashmore, M. Bustamante, S. Cinderby, E. Davidson, F. Dentener, B. Emmett, J.-W. Erisman, M. Fenn, F. Gilliam, A. Nordin, L. Pardo, W. De Vries, *Ecol. Appl.* **2010**, *20*, 30, <https://doi.org/10.1890/08-1140.1>.
- [9] K. Butterbach-Bahl, E.M. Baggs, M. Dannenmann, R. Kiese, S. Zechmeister-Boltenstern, *Phil. Trans. Roy. Soc. B* **2013** *368*, 20130122. <https://doi.org/10.1098/rstb.2013.0122>.
- [10] T. Bühlmann, E. Hiltbrunner, C. Körner, B. Rihm, B. Achermann, *Atmos. Environ.* **2015**, *103*, 94. <https://doi.org/10.1016/j.atmosenv.2014.12.037>.
- [11] UNECE, 'The 1999 Gothenburg Protocol to Abate Acidification, Eutrophication and Ground-level Ozone', **1999**, [http://www.unece.org/env/lrtap/multi\\_h1.html](http://www.unece.org/env/lrtap/multi_h1.html).
- [12] C. Häni, J. Sintermann, T. Kupper, M. Jocher, A. Neftel, *Atmos. Environ.* **2016**, *125*, 92. <https://doi.org/10.1016/j.atmosenv.2015.10.069>.
- [13] I. Trebs, C. Ammann, J. Junk, 'Springer Handbook of Atmospheric Measurements', Ed. T. Foken, Springer, Cham, **2021**, p. 1445.
- [14] E. Seitler, M. Meier, 'Ammoniak-Immissionsmessungen in der Schweiz 2000 bis 2022', Forschungsstelle für Umweltbeobachtung (FUB), **2023**, <https://www.bafu.admin.ch/bafu/de/home/themen/luft/publikationen-studien/studien.html>.
- [15] J. Mohn, K. Zeyer, M. Keck, M. Keller, M. Zähler, J. Poteko, L. Emmenegger, S. Schrade, *Atmos. Environ.* **2018**, *179*, 12, <https://doi.org/10.1016/j.atmosenv.2018.01.057>.
- [16] J. Sintermann, K. Dietrich, C. Häni, M. Bell, M. Jocher, A. Neftel, *Atmos. Meas. Tech.* **2016**, *9*, 2721. <https://doi.org/10.5194/amt-9-2721-2016>.
- [17] J. Sintermann, A. Neftel, C. Ammann, C. Häni, A. Hensen, B. Loubet, C. R. Flechard, *Biogeosciences* **2012**, *9*, 1611.
- [18] H. Menzi, P. E. Katz, M. Fahrni, A. Neftel, R. Frick, *Atmos. Environ.* **1998**, *32*, 301. [http://doi.org/10.1016/s1352-2310\(97\)00239-2](http://doi.org/10.1016/s1352-2310(97)00239-2).
- [19] J. Sintermann, C. Ammann, U. Kuhn, C. Spirig, R. Hirschberger, A. Gärtner, A. Neftel, *Atmos. Meas. Tech.* **2011**, *4*, 1821, <https://doi.org/10.5194/amt-4-1821-2011>.
- [20] K. Voglmeier, M. Jocher, C. Häni, C. Ammann, *Biogeosciences* **2018**, *15*, 4593, <https://doi.org/10.5194/bg-15-4593-2018>.
- [21] C. Spirig, C. R. Flechard, C. Ammann, A. Neftel, *Biogeosciences* **2010**, *7*, 521, <https://doi.org/10.5194/bg-7-521-2010>.
- [22] J. Sintermann, C. Spirig, A. Jordan, U. Kuhn, C. Ammann, A. Neftel, *Atmos. Meas. Tech.* **2011**, *4*, 599, <https://doi.org/10.5194/amt-4-599-2011>.
- [23] N. W. M. Ogink, J. Mosquera, S. Calvet, G. Zhang, *Biosyst. Eng.* **2013**, *116*, 297, <https://doi.org/10.1016/j.biosystemseng.2012.10.005>.
- [24] T. K. Flesch, L. A. Harper, J. M. Powell, J. D. Wilson, *Trans. ASABE*, **2009**, *52*, 253. <https://doi.org/10.13031/2013.25946>.
- [25] A. C. Valach, C. Häni, M. Bühler, J. Mohn, S. Schrade, T. Kupper, *J. Air. Waste. Manag. Assoc.* **2023**, *73*, 930, <https://doi.org/10.1080/10962247.2023.2271426>.
- [26] Agrammon, <https://www.agrammon.ch>, accessed April 30, 2024.
- [27] T. Kupper, C. Bonjour, H. Menzi, *Atmos. Environ.* **2015**, *103*, 215, <https://doi.org/10.1016/j.atmosenv.2014.12.024>.
- [28] B. Rihm, B. Achermann, 'Critical Loads of Nitrogen and their Exceedances. Swiss contribution to the effects-oriented work under the Convention on Long-range Transboundary Air Pollution (UNECE)', Federal Office for the Environment, Bern, **2016**.
- [29] B. Rihm, T. Künzle, 'Nitrogen deposition and exceedances of critical loads for nitrogen in Switzerland 1990–2020', **2023**, <https://www.bafu.admin.ch/bafu/en/home/topics/air/publications-studies/studies.html>, accessed April 30, 2024.
- [30] S. Schrade, K. Zeyer, J. Mohn, M. Zähler, *Sci. Total Environ.* **2023**, *896*, 165027. <https://doi.org/10.1016/j.scitotenv.2023.165027>.
- [31] UNECE, 'Guidance document on preventing and abating ammonia emissions from agricultural sources', United Nations Economic Commission for Europe, Executive Body for the Convention on Long-range Transboundary Air Pollution, ECE/EB.AIR/120, **2014**.
- [32] R. M. Hoesly, S. J. Smith, L. Feng, Z. Klimont, G. Janssens-Maenhout, T. Pitkanen, J. J. Seibert, L. Vu, R. J. Andres, R. M. Bolt, T. C. Bond, L. Dawidowski, N. Kholod, J.-I. Kurokawa, M. Li, L. Liu, Z. Lu, M. C. Moura, P. R. O'Rourke, Q. Zhang, *Geosci. Model Dev.* **2018**, *11*, 369, <https://doi.org/10.5194/gmd-11-369-2018>.
- [33] E. Dammers, C. A. McLinden, D. Griffin, M. W. Shephard, S. Van Der Graaf, E. Lutsch, M. Schaap, Y. Gainairu-Matz, V. Fioletov, M. Van Damme, S. Whitburn, L. Clarisse, K. Cady-Pereira, C. Clerbaux, P. F. Coheur, J. W. Erisman, *Atmos. Chem. Phys.* **2019**, *19*, 12261, <https://doi.org/10.5194/acp-19-12261-2019>.
- [34] R. Abeer, C. Viatte, W. C. Porter, N. Evangelio, C. Clerbaux, L. Clarisse, M. Van Damme, P.-F. Coheur, S. Safieddine, *Atmos. Chem. Phys.* **2023**, *23*, 12505, <https://doi.org/10.5194/acp-23-12505-2023>.
- [35] S. J. Pai, C. L. Heald, J. G. Murphy, *ACS Earth and Space Chem.* **2021**, *5*, 1674, <https://doi.org/10.1021/acsearthspacechem.1c00021>.
- [36] A. Nenes, S. N. Pandis, R. J. Weber, A. Russell, *Atmos. Chem. Phys.* **2020**, *20*, 3249, <https://doi.org/10.5194/acp-20-3249-2020>.
- [37] A. Nenes, S. N. Pandis, M. Kanakidou, A. G. Russell, S. Song, P. Vasilakos, R. J. Weber, *Atmos. Chem. Phys.* **2021**, *21*, 6023, <https://doi.org/10.5194/acp-21-6023-2021>.
- [38] C. Fountoukis, A. Nenes, *Atmos. Chem. Phys.* **2007**, *7*, 4639, <https://doi.org/10.5194/acp-7-4639-2007>.
- [39] C. Spirig, A. Neftel, *Agrarforschung* **2006**, *13*, 392.
- [40] S. Aksoyoglu, J. Keller, I. Barmpadimos, D. Oderbolz, V. A. Lanz, A. S. H. Prévôt, U. Baltensperger, *Atmos. Chem. Phys.* **2011**, *11*, 7355, <https://doi.org/10.5194/acp-11-7355-2011>.
- [41] S. Aksoyoglu, J. Keller, G. Ciarelli, A. S. H. Prévôt, U. Baltensperger, *Atmos. Chem. Phys.* **2014**, *14*, 13081, <https://doi.org/10.5194/acp-14-13081-2014>.
- [42] S. Aksoyoglu, J. Jiang, G. Ciarelli, U. Baltensperger, A. S. H. Prévôt, *Atmos. Chem. Phys.* **2020**, *20*, 15665, <https://doi.org/10.5194/acp-20-15665-2020>.
- [43] S. K. Grange, J. Sintermann, C. Hueglin, *Sci. Total Environ.* **2023**, *900*, 165844, <https://doi.org/10.1016/j.scitotenv.2023.165844>.
- [44] A. Valach, C. Häni, T. Kupper, 'Einfluss der jährlichen Temperaturschwankungen auf die modellierten Ammoniakemissionen der Tierproduktion von 2002 bis 2019', **2023**.
- [45] C. R. Flechard, E. Nemitz, R. I. Smith, D. Fowler, A. T. Vermeulen, A. Bleeker, J. W. Erisman, D. Simpson, L. Zhang, Y. S. Tang, M. A. Sutton, *Atmos. Chem. Phys.* **2011**, *11*, 2703, <https://doi.org/10.5194/acp-11-2703-2011>.
- [46] A. Fischer-Riedmann, PhD Thesis ETH Zürich No. 11035, **1995**.
- [47] R. Hesterberg, A. Blatter, M. Fahrni, M. Rosset, A. Neftel, W. Eugster, H. Wanner, *Environ. Pollut.* **1996**, *91*, 21, [https://doi.org/10.1016/0269-7491\(95\)00036-Q](https://doi.org/10.1016/0269-7491(95)00036-Q).
- [48] C. R. Flechard, C. Spirig, A. Neftel, C. Ammann, *Biogeosciences* **2010**, *7*, 537, <https://doi.org/10.5194/bg-7-537-2010>.
- [49] V. Wolff, I. Trebs, C. Ammann, F. X. Meixner, *Atmos. Meas. Tech.* **2010**, *3*, 187, <https://doi.org/10.5194/amt-3-187-2010>.
- [50] U. Zöll, C. Brümmer, F. Schrader, C. Ammann, A. Ibrom, C. R. Flechard, D. Nelson, M. Zahniser, W. L. Kutsch, *Atmos. Chem. Phys.* **2016**, *16*, 11283, <https://doi.org/10.5194/acp-16-11283-2016>.
- [51] D. Pan, K. B. Benedict, L. M. Golston, R. Wang, J. L. Collett Jr., L. Tao, K. Sun, X. Guo, J. Ham, A. J. Prenni, B. A. Schichtel, T. Mikoviny, M. Müller, A. Wisthaler, M. A. Zondlo, *Environ. Sci. Technol.* **2021**, *55*, 7776, <https://doi.org/10.1021/acs.est.0c05749.s001>.
- [52] S. Braun, B. Ahrends, R. Alonso, S. Augustin, H. García-Gómez, I. Hunová, P. E. Karlsson, G. P. Karlsson, A. Schmitz, A. Thimonier, *Front. For. Glob. Change* **2022**, *5*, <https://doi.org/10.3389/ffgc.2022.1062223>.
- [53] A. Thimonier, M. Schmitt, P. Waldner, B. Rihm, *Environ. Monit. Assess.* **2005**, *104*, 81, <https://doi.org/10.1007/s10661-005-1605-9>.
- [54] M. Schmitt, L. Thöni, P. Waldner, A. Thimonier, *Atmos. Environ.* **2005**, *39*, 1079, <https://doi.org/10.1016/j.atmosenv.2004.09.075>.
- [55] E. Wortman, T. Tomaszewski, P. Waldner, P. Schleppei, A. Thimonier, W. Eugster, N. Buchmann, H. Sievering, *Tellus* **2012**, *B 64*, 17216, <http://doi.org/17210.13402/tellusb.v17264i17210.17216>.
- [56] B. Rihm B., T. Künzle, 'Mapping Nitrogen Deposition 2015 for Switzerland', **2019**, <https://www.bafu.admin.ch/bafu/en/home/topics/air/publications-studies/studies.html>, accessed April 30, 2024.
- [57] Federal Office for the Environment (FOEN), 'Luftqualität 2021. Messresultate des Nationalen Beobachtungsnetzes für Luftfremdstoffe (NABEL)', **2022**, <http://www.bafu.admin.ch/uz-2114-d>, accessed April 30, 2024.
- [58] A. Thimonier, Z. Kosonen, S. Braun, B. Rihm, P. Schleppei, M. Schmitt, E. Seitler, P. Waldner, L. Thöni, *Atmos. Environ.* **2019**, *198*, 335, <http://doi.org/10.1016/j.atmosenv.2018.10.051>.
- [59] S. Aksoyoglu, and A. S. H. Prévôt, *Int. J. Environ. Pollut.* **2018**, *64*, 230, <https://doi.org/10.1504/IJEP.2018.10020573>.
- [60] J. Heldstab, F. Leppert, R. Biedermann, O. Schwank, 'Stickstoffflüsse in der Schweiz 2020. Stoffflussanalyse und Entwicklungen. Bundesamt für Umwelt', **2013**, [www.bafu.admin.ch/uh-1309-d](https://www.bafu.admin.ch/uh-1309-d), accessed April 30, 2024.
- [61] H. Klein, M. Gauss, S. Tsyro, A. Nyíri, 'Transboundary air pollution by sulphur, nitrogen, ozone and particulate matter in 2021. Switzerland', Norwegian Meteorological Institute. MSC-W Data Note 1/2023, **2023**.
- [62] L. Zhang, J. R. Brook, R. Vet, *Atmos. Chem. Phys.* **2003**, *3*, 2067, <https://doi.org/10.5194/acp-3-2067-2003>.
- [63] M. A. Sutton, J. K. Burkhardt, D. Guerin, E. Nemitz, D. Fowler, *Atmos. Environ.* **1998**, *32*, 473, [https://doi.org/10.1016/s1352-2310\(97\)00164-7](https://doi.org/10.1016/s1352-2310(97)00164-7).
- [64] R. J. Wichink Kruit, M. Schaap, F. J. Sauter, M. C. van Zanten, W. A. J. van Pul, *Biogeosciences* **2012**, *9*, 5261, <https://doi.org/10.5194/bg-9-5261-2012>.
- [65] R.-S. Massad, E. Nemitz, M. A. Sutton, *Atmos. Chem. Phys.* **2010**, *10*, 10359, <https://doi.org/10.5194/acp-10-10359-2010>.
- [66] L. J. Sheppard, I. D. Leith, T. Mizunuma, J.N. Cape, A. Crossley, S. Leeson, M. A. Sutton, D. Fowler, N. van Dijk, *Global Change Bio.* **2011**, *17*, 3589, <https://doi.org/10.1111/j.1365-2486.2011.02478.x>.
- [67] A. G. Deshpande, M. R. Jones, N. van Dijk, N. J. Mullinger, D. Harvey, R. Nicoll, G. Toteva, G. Weerakoon, S. Nissanka, B. Weerakoon, M.



- Grenier, A. Iwanicka, F. Duarte, A. Stephens, C. J. Ellis, M. Vieno, J. Drewer, P. A. Wolsey, S. Nanayakkara, T. Prabhawara, W. J. Bealey, E. Nemitz, M. A. Sutton, *Atmos. Environ.* **2024**, *320*, 120325, <https://doi.org/10.1016/j.atmosenv.2023.120325>.
- [68] S. Bassin, M. Volk, J. Fuhrer, *Ecosystems* **2013**, *16*, 1105, <https://doi.org/10.1007/s10021-013-9670-3>.
- [69] T. Roth, L. Kohli, B. Rihm, B. Achermann, *Agric. Ecosys. Environ.* **2013**, *178*, 121, <https://doi.org/10.1016/j.agee.2013.07.002>.
- [70] S. Braun, S. Tresch, S. Augustin, *Plos One* **2020**, *15*, e0227530, <https://doi.org/10.1371/journal.pone.0227530>.
- [71] M. Jonard, A. Fürst, A. Verstraeten, A. Thimonier, V. Timmermann, N. Potočić, P. Waldner, S. Benham, K. Hansen, P. Merilä, Q. Ponette, A. C. de la Cruz, P. Roskams, M. Nicolas, L. Croisé, M. Ingerslev, G. Matteucci, B. Decinti, M. Bascietto, P. Rautio, *Glob. Change Bio.* **2015**, *21*, 418, <https://doi.org/10.1111/gcb.12657>.
- [72] S. Braun, C. Schindler, B. Rihm, *Front. For. Glob. Change* **2020**, *3*, <https://doi.org/10.3389/ffgc.2020.00033>.
- [73] S. Braun, C. Schindler, R. Volz, W. Flückiger, *Water Air Soil Pollut.* **2003**, *142*, 327, <https://doi.org/10.1023/A:1022088806060>.
- [74] V. Blanke, S. Bassin, M. Volk, J. Fuhrer, *Acta Oecol.* **2012**, *45*, 57, <https://doi.org/10.1016/j.actao.2012.09.002>.
- [75] L. C. de Witte, N. P. Rosenstock, S. van der Linde, S. Braun, *Sci. Tot. Environ.* **2017**, *605*, 1083, <https://doi.org/10.1016/j.scitotenv.2017.06.142>.
- [76] S. van der Linde, L. M. Suz, C. D. L. Orme, F. Cox, H. Andreae, E. Asi, B. Atkinson, S. Benham, C. Carroll, N. Cools, B. De Vos, H.-P. Dietrich, J. Eichhorn, J. Gehrmann, T. Grebenc, H. S. Gweon, K. Hansen, F. Jacob, F. Kristöfel, P. Lech, M. Manninger, J. Martin, H. Meeseburg, P. Merilä, M. Nicolas, P. Pavlenda, P. Rautio, M. Schaub, H.-W. Schröck, W. Seidling, V. Šrámek, A. Thimonier, I. M. Thomsen, H. Titeux, E. Vanguelova, A. Verstraeten, L. Vesterdal, P. Waldner, S. Wijk, Y. Zhang, D. Žlindra, M. I. Bidartondo, *Nature* **2018**, *558*, 243, <https://doi.org/10.1038/s41586-018-0189-9>.
- [77] B. Rohner, P. Waldner, H. Lischke, M. Ferretti, E. Thürig, *Eur. J. For. Res.* **2017**, *137*, 29, <https://doi.org/10.1007/s10342-017-1087-7>.
- [78] S. Etzold, M. Ferretti, G. J. Reinds, S. Solberg, A. Gessler, P. Waldner, M. Schaub, D. Simpson, S. Benham, K. Hansen, M. Ingerslev, M. Jonard, P. E. Karlsson, A.-J. Lindroos, A. Marchetto, M. Manninger, H. Meeseburg, P. Merilä, P. Nöjd, P. Rautio, T. G. M. Sanders, W. Seidling, M. Skudnik, A. Thimonier, A. Verstraeten, L. Vesterdal, M. Vejvustkova, W. de Vries, *For. Ecolo. Manag.* **2020**, *458*, 117762, <https://doi.org/10.1016/j.foreco.2019.117762>.
- [79] M. Ferretti, M. Calderisi, A. Marchetto, P. Waldner, A. Thimonier, M. Jonard, N. Cools, P. Rautio, N. Clarke, K. Hansen, P. Merilä, and N. Potočić, *An. For. Sci.* **2015**, *72*, 897, <https://doi.org/10.1007/s13595-014-0445-6>.
- [80] CLRTAP, 'Manual on methodologies and criteria for modelling and mapping critical loads and levels and air pollution effects, risks and trends', Final Report, UNECE Convention on Long-range Transboundary Air Pollution, German Environment Agency, Texte 109/2023, **2023**.
- [81] R. Bobbink, R., C. Loran, H. Tomassen, 'Review and revision of empirical critical load of nitrogen for Europe', German Environment Agency, Dessau-Rosslau, Germany, **2022**, <https://www.umweltbundesamt.de/en/publikationen/review-revision-of-empirical-critical-loads-of>, accessed April 30, 2024.
- [82] T. Spranger, R. Smith, D. Fowler, G. Mills, M. Posch, J. Hall, G. Schütze, J.-P. Hettelingh, J. Slootweg, 'Modelling and Mapping Critical Loads and Levels and Air Pollution Effects, Risks and Trends', **2004**, [www.icpmap-ping.org](http://www.icpmap-ping.org), accessed April 30, 2024.
- [83] P. Waldner, A. Thimonier, E. Graf Pannatier, S. Etzold, M. Schmitt, A. Marchetto, P. Rautio, K. Derome, T. M. Nieminen, S. Nevalainen, A. J. Lindroos, P. Merilä, G. Kindermann, M. Neumann, N. Cools, B. de Vos, P. Roskams, A. Verstraeten, K. Hansen, G. Pihl Karlsson, H.-P. Dietrich, S. Raspe, R. Fischer, M. Lorenz, S. Iost, O. Granke, T. G. M. Sanders, A. Michel, H. D. Nagel, T. Scheuschner, P. Simoncic, K. von Wilpert, H. Meeseburg, S. Fleck, S. Benham, E. Vanguelova, N. Clarke, M. Ingerslev, L. Vesterdal, P. Gundersen, I. Stupak, M. Jonard, N. Potočić, M. Minaya, *An. For. Sci.* **2015**, *72*, 929, <https://doi.org/10.1007/s13595-015-0489-2>.
- [84] Z. Kosonen, E. Schnyder, E. Hiltbrunner, A. Thimonier, M. Schmitt, E. Seitler, L. Thöni, *Atmos. Environ.* **2019**, *211*, 214, <https://doi.org/10.1016/j.atmosenv.2019.05.005>.
- [85] J. Franzaring, J. Köslér, 'Review of internationally proposed critical levels for ammonia'. Proceedings of an Expert Workshop held in Dessau and online on 28/29 March **2022**, German Environment Agency, Texte 31/2023, 2023.
- [86] EKL, 'Ammoniak-Immissionen und Stickstoffeinträge, Abklärungen der EKL zur Beurteilung der Übermässigkeit', Eidgenössische Kommission für Lufthygiene EKL, **2014**, <https://www.ekl.admin.ch/de/dokumentation/publikationen>, accessed April 30, 2024.
- [87] K. Wang, P. Kang, Y. Lu, X. Zheng, M. Liu, T.-J. Lin, K. Butterbach-Bahl, Y. Wang, *Agric. For. Meteorology* **2021**, *308*, 108570, <https://doi.org/10.1016/j.agrformet.2021.108570>.
- [88] D. Swart, J. Zhang, S. van der Graaf, S. Rutledge-Jonker, A. Hensen, S. Berkhout, P. Wintjen, R. van der Hoff, M. Haaima, A. Frumau, P. van den Bulk, R. Schulte, M. van Zanten, T. van Goethem, *Atmos. Meas. Techniques* **2023**, *16*, 529; <https://doi.org/10.5194/amt-16-529-2023>.
- [89] ReCLEAN <https://recclean.epfl.ch/the-project>, accessed April 30, 2024.
- [90] HAFL <https://www.bfh.ch/en/research/research-projects/2024-092-697-633>, accessed April 30, 2024.

#### License and Terms



This is an Open Access article under the terms of the Creative Commons Attribution License CC BY 4.0. The material may not be used for commercial purposes.

The license is subject to the CHIMIA terms and conditions: (<https://chimia.ch/chimia/about>).

The definitive version of this article is the electronic one that can be found at <https://doi.org/10.2533/chimia.2024.771>